Charge transfer at double-layer to single-layer transition in double-quantum-well systems

Y. Katayama,* D. C. Tsui, H. C. Manoharan, S. Parihar, and M. Shayegan
Department of Electrical Engineering, Princeton University, Princeton, New Jersey 08544
(Received 3 August 1993; revised manuscript received 31 May 1994)

Experiments on an abrupt double-layer to single-layer transition in double-quantum-well structures are presented. This transition of an electronic system is observed as a sharp decresae in resistance when the top gate is negatively biased. Data on the Shubnikov–de Haas oscillations taken at different gate voltages show that this abrupt decrease in resistance occurs when the system changes from being double-layer to single-layer and is accompanied by transferring of electrons from the top to the bottom layer. A phenomenological model is developed to explain the transition and its dependence on the barrier width of the sample. We also find that the strength of interlayer Coulomb scattering is significantly enhanced before the transition.

I. INTRODUCTION

Recently, electron transport experiments in two parallel two-dimensional electron gases (2DEG's) have been of wide interest. Such a system allows different types of measurements which were not accessible with a single 2DEG. These experiments include effects due to interlayer tunneling,[1–4] interlayer Coulomb scattering,[5,6] and new types of integer and fractional quantum Hall effects.[7–10] In addition, it is expected that small interlayer spacings comparable to or even smaller than the intralayer mean electron distance can cause instability in electron densities in the wells. This expectation is based on the fact that the Coulomb interaction between electrons in the same layer can be significantly reduced due to Pauli's exclusion principle, while that between electrons in different layers can remain large since the wave functions overlap little in the z direction. Theoretically, the instability has been discussed in the context of the one due to exchange effects[11,12] or in a broader context, as a charge-transfer instability in the extended multiband Hubbard model.[13–17]

Here, we report data on an abrupt double-layer to single-layer transition in GaAs-AlAs double-quantum-well (DQW) structures,[18] which we believe cannot be explained within a single-particle model. This transition of an electronic system is seen as a sharp four-terminal resistance drop when the top gate is negatively biased, accompanied by a rapid change in the Shubnikov–de Haas (SdH) oscillations from being double-layer to single-layer. For samples of thinner and thicker AlAs barriers, the feature in resistance becomes weaker and the rapid change in the SdH oscillations is less obvious. On the basis of the above experimental facts, a phenomenological model is developed to give a possible explanation of the transition and its dependence on the barrier width of the sample. We also find that the interlayer Coulomb scattering before the transition is significantly enhanced compared to that extrapolated from previous studies[5,19,20] in order to explain the amount of our resistance decrease. Possible reasons for this enhancement are discussed.

II. EXPERIMENT

Three GaAs-AlAs DQW samples are studied, each with a different AlAs barrier width ($M229$, 14 Å; $M293$, 70 Å; $MM10$, 100 Å) sandwiched between two 150-Å (for $M229$ 180-Å) GaAs wells. The samples we measured here have total electronic densities of 2.6×10^{11}, 3.2×10^{11}, and $2.3\times10^{11}/\mathrm{cm}^2$ supplied from top and bottom δ-doping layers, and mobilities of 3.2×10^5, 8.4×10^5, and 8.3×10^4 $\mathrm{cm}^2/\mathrm{V\,s}$, respectively, when the wells are balanced. The choice of a pure AlAs barrier significantly reduces the tunneling between the two layers compared to an $Al_xGa_{1-x}As$ barrier with the same thickness while keeping the interlayer Coulomb interactions the same. The estimated energy gaps, Δ_{SAS}'s, between the symmetric and antisymmetric states are ~10 K for $M229$, ~0.01 K for $M293$, and negligibly small for $MM10$. Both H-shape mesa and standard Hall bar structures with an Al Schottky gate covering an active region of ~100 $\mu\mathrm{m}^2$ were fabricated. The resistance was measured in the four-terminal configuration as a function of the gate voltage V_g using the standard lock-in detection technique. A constant current excitation of 10 nA at 13 Hz was used throughout the measurement. The experiment was conducted using a ^{3}He cryostat.

III. DATA

Figures 1(a)–1(c) display our main results from the four-terminal resistance vs V_g measurements at $B=0$ on the three samples. Note that the data taken at different T's in Figs. 1(b) and 1(c) are displaced for clarity.

Sample $M229$ with a 14-Å AlAs barrier shows a smooth change in resistance. The increasing resistance when V_g is negatively biased is expected and has two causes: One is the decrease in the carrier densities and the other is the increase in scattering rate. Around $V_g\sim-0.5$ V, a small slope change in the resistance curve, which indicates something more than the above simple scenario, is discernible. In order to amplify this feature, the derivative dR/dV_g is calculated from the

resistance data and is shown as the dotted curve in Fig. 1(a). A broad peak in dR/dV_g is clearly seen around $V_g = -0.5$ V. Further negatively biasing the well does not give any noticeable features.

The data taken on sample $M293$, which has a 70-Å AlAs barrier, are shown in Fig. 1(b). At $T = 0.3$ K, a sudden resistance decrease of more than 50% starts at $V_g \sim -0.44$ V. Since this large resistance decrease is unexpected when the carrier density of the sample is decreasing continuously, we have repeated the measurement on the same piece of the sample after different thermal cycles and also on different pieces of the sample. The feature is consistently observed in every measurement, though the magnitude and sharpness of the decrease sometimes vary. While further reduction in T does not change the data much, the feature weakens with increasing T. At $T = 15$ K, the feature is already quite broad and at $T = 77$ K, no feature is observed. From these data, we estimate that the characteristic energy scale of the transition for this sample is a few meV.

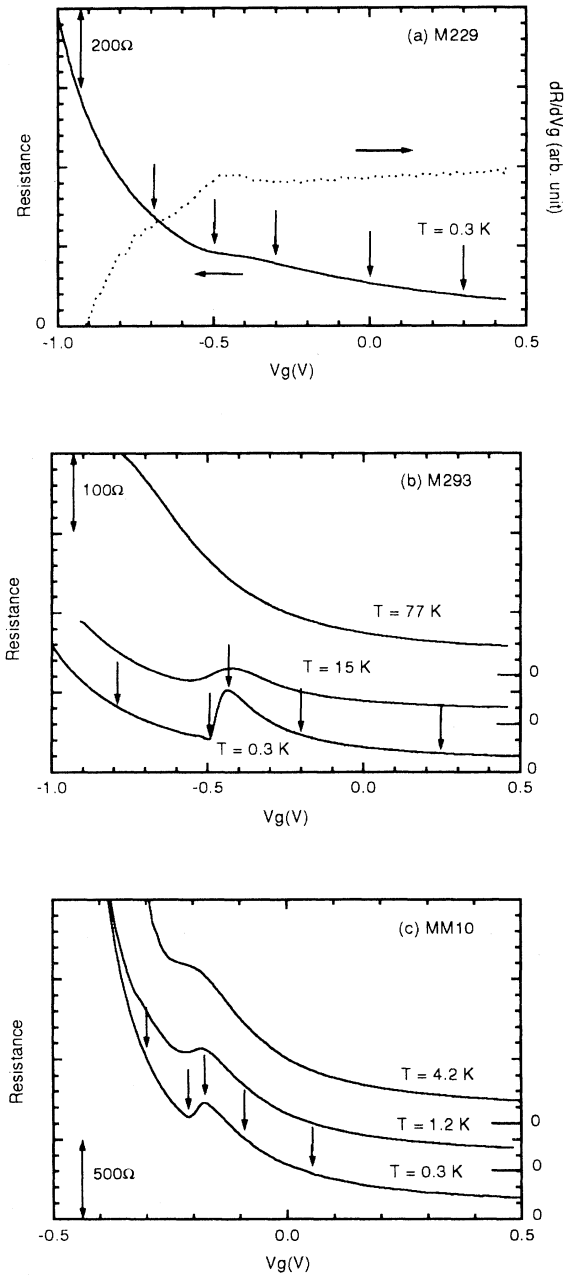

FIG. 1. Four-terminal resistance as a function of V_g at $B = 0$ for three samples: (a) $M229$, (b) $M293$, and (c) $MM10$. Vertical arrows indicate the positions of V_g's at which the SdH oscillations are displayed in Fig. 2. Note that data at different T's are displaced for clarity by 15%. The dotted line for $M229$ is the derivative.

Further increasing the barrier thickness weakens the feature. As is seen in the $T = 0.3$ K trace in Fig. 1(c), the third sample $MM10$ with the largest barrier (100 Å) shows a considerably weaker and smoother resistance decrease starting at $V_g \sim -0.18$ V. The characteristic energy scale for this sample is less than 1 meV [see $T = 1.2$ and 4.2 K traces in Fig. 1(c)]. Note that in this case, since the distance between the 2DEG's and the top gate is the smallest among the three samples, the density changes much faster as a function of V_g.

Let us mention a few side remarks. First, all the data were taken by sweeping down V_g. The quality of the data taken by sweeping up V_g is usually slightly worse, showing small bumps superimposed on the main feature, due to some inhomogeneity resulting from the large negative biases. These small bumps are easily distinguished from the main feature since they occur at random V_g's. Second, a sharp resistance drop is observed for different pieces of $M293$ with different mobilities (ranging from 3×10^5 to 1×10^6 cm^2/V s). Considering that we also see the feature in the low-mobility sample $MM10$, it seems that the feature in resistance is rather insensitive to impurity scattering. Third, the feature becomes weaker for a van der Pauw piece of the sample $M293$ with a much larger active area (>4 mm^2), suggesting that the feature is very sensitive to macroscopic inhomogeneity across the active region.

The feature in resistance is further studied by taking the SdH oscillations in R_{xx} at low B fields at different V_g's and by extracting the density information. Figures 2(a)–2(c) show the data taken at the V_g's indicated by the vertical arrows in Figs. 1(a)–1(c). The densities, n_1 and n_2, of the higher and lower subbands of the DQW's as a function of V_g, are derived by Fourier transforming the SdH oscillations and the results are presented in Figs. 3(a)–3(c). We note that when the energies of the states in the individual wells differ by less than Δ_{SAS}, the stationary states are delocalized over the wells and n_1 and n_2 correspond to the densities in the antisymmetric and symmetric subbands, and when the energies differ by more than Δ_{SAS}, the states are localized in the individual wells and n_1 and n_2 correspond to the densities of the top and bottom wells. In all three samples, the results demonstrate that the feature (whether it is abrupt or smooth) observed in Figs. 1(a)–1(c) occurs when n_1 goes to zero, i.e., the system changes from being double layer to single layer. We now examine the data for each sam-

ple in greater detail in the rest of this section.

The SdH oscillation patterns for $M229$ in Fig. 2(a) change smoothly from two-subband-like to single-subband-like when V_g is negatively biased. At $V_g=0.3$ V, where the densities of the two quantum wells are balanced, the stationary states of the system are the symmetric and antisymmetric states generated by the symmetric and antisymmetric linear combinations of the states in the individual wells. The density difference of these states due to Δ_{SAS} gives rise to the observed beating. For a large imbalance of the wells, the stationary states are localized in the individual wells. Thus, the beating comes from the density difference between the individual wells. Further biasing V_g completely deplete the top well at $V_g \sim -0.5$ V and the beating disappears. The SdH oscillations become less well resolved at large negative V_g's since the mobility of the sample becomes lower.

The result on n_1, n_2, and their average, n_{av}, from the Fourier transforms are shown in Fig. 3(a). It demonstrates beautifully what we expect from single-particle quantum mechanics.[21] Since the Fermi levels of the two subbands are equal, the difference in carrier density in the two states represents the difference in energy of the subband edges. Δ_{SAS} derived from the minimum density difference at $V_g=0.3$ V is 9 K. This result gives a rough voltage scale to determine whether the electron states are localized or delocalized. In the case for $M229$, it is ~ 0.2 V in the scale of V_g. When $V_g > 0.3+0.2$ V, the lower subband is localized in the top well and the upper subband is localized in the bottom well. Changing V_g mostly changes the lower subband density n_2 in the top well [except for the slight change in n_1 due to the field penetration of the 2DEG (Ref. 22)]. When V_g approaches 0.3 V, the states localized in the two wells transform to the states delocalized over the wells. Now the lower subband is the symmetric combination of the states localized in each well while the upper subband is the antisymmetric combination. If $V_g < 0.3-0.2$ V, the lower subband is

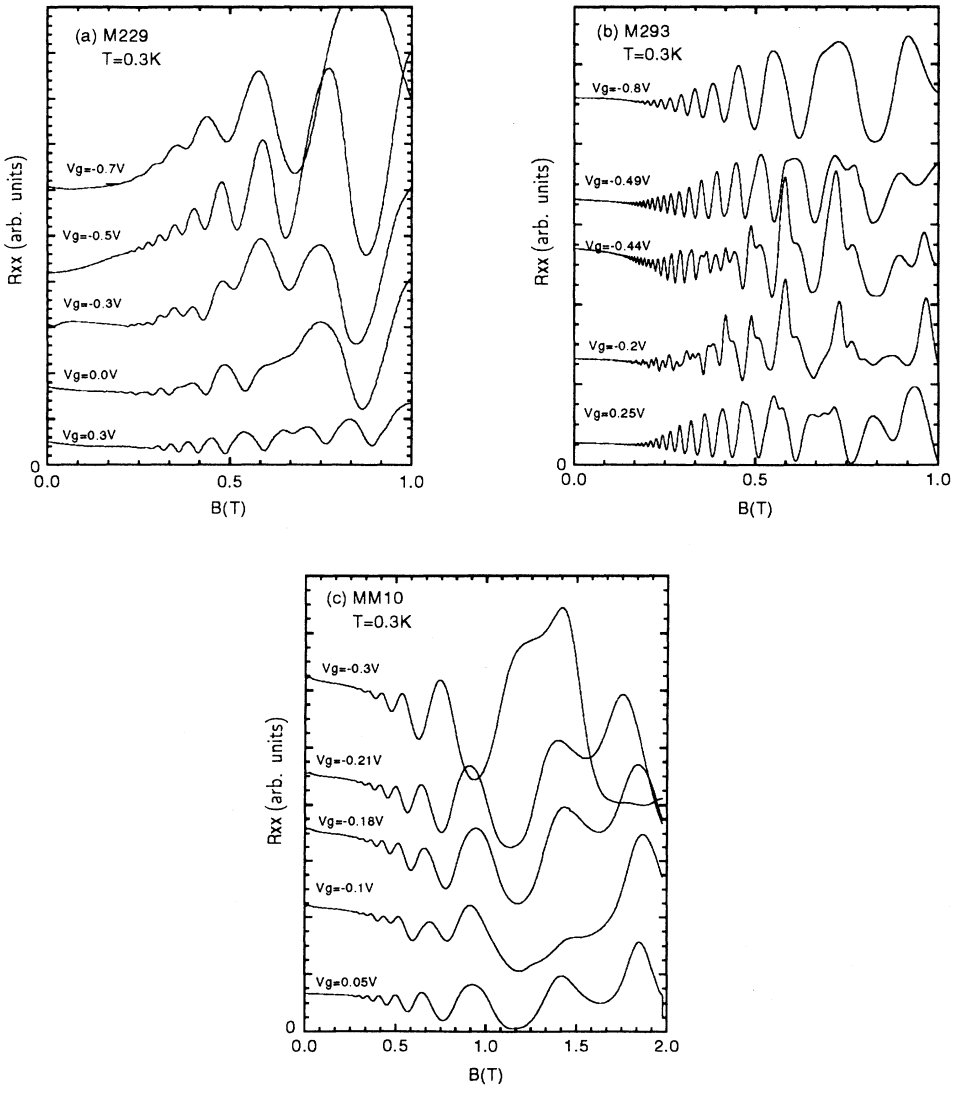

FIG. 2. SdH oscillations at different V_g's for three samples taken at $T=0.3$ K. Data in each figure are in a same scale but displaced by one major tick: (a) $M229$; (b) $M293$; (c) $MM10$.

localized to the bottom well and the upper to the top well. Consequently, changing V_g changes the upper subband density n_1 now in the top well. The density of the top well becomes zero at $V_g \sim -0.6$ V. At still higher negative bias, the system is a single-layer 2DEG. It should be noted that the averaged density $n_{av}=(n_1+n_2)/2$ changes approximately linearly with V_g, as is expected from Gauss's law.

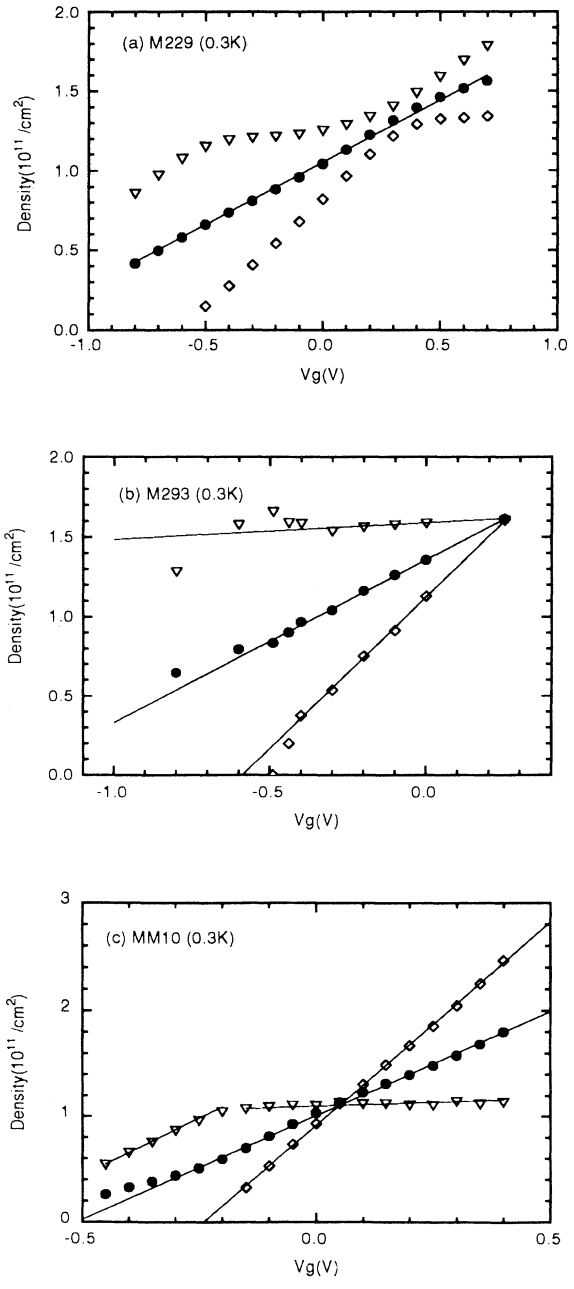

FIG. 3. Densities derived from the Fourier transforms of the SdH oscillations as a function of V_g: ◇, n_1; ▽, n_2; ●, n_{av}. Note that n_1 at $V_g=0.49$ V is not from the Fourier transform but given as a reference point.

For sample $M293$, the SdH oscillations in Fig. 2(b) show that the system changes suddenly from a double-layer to a single-layer at the V_g where the sudden resistance decrease is observed in Fig. 1(b). At $V_g=0.25$ V, the single-frequency oscillations show that the densities are balanced. In this sample, Δ_{SAS} is too small to give measurable density difference between n_1 and n_2. As V_g decreases, the wells become off balanced and the beating shows up, due to the density difference between n_1 and n_2. This beating disappears suddenly at $V_g=-0.49$ V, at the abrupt change in resistance seen in Fig. 1(b). The beating structure at $V_g=-0.44$ V, where the densities of the two wells are expected to be far off balanced, is a result of the nonlinear coupling between two frequencies in two-subband systems discussed in Refs. 23 and 24.

The n_1, n_2, and n_{av} data in Fig. 3(b) shows that there is a charge transfer from the top to the bottom well at the transition. Starting at $V_g \sim -0.4$ V, n_1 drops sharply to zero, while n_2 shows more than a 10% increase. The n_{av}, on the other hand, keeps changing linearly with V_g. After the top well is completely depleted, n_{av} decreases more slowly, consistent with the change in the lever arm factor in the capacitance network model,[25] as a result of a larger distance between the bottom 2DEG and the top gate. The weak decrease in n_2, when $n_1>0$, is due to the imperfect screening of the top 2DEG.[22]

The SdH oscillations for $MM10$ in Fig. 2(c) exhibit behavior similar to that of the SdH oscillations for $M293$, even though they are less clear due to the lower mobility of the sample. The system changes from being double-layer to single-layer between $V_g=-0.18$ and -0.21 V, corresponding to the resistance drop in Fig. 1(c). However, it is difficult to identify the charge transfer from the density data in Fig. 3(c), because of the weaker transition in Fig. 1(c) and the lower resolution of the SdH oscillations. On the other hand, the slope change in n_{av} after the top well is depleted is most pronounced among the three samples. This is because of the larger distance between the wells giving rise to a larger change in the capacitance.

IV. DISCUSSION

Before starting the discussion, we summarize the experimental results presented in the last section: (1) We observe a feature in the four-terminal resistance when the system changes from a double- to a single-layer system. (2) The feature is smooth for $M229$, while it is a very abrupt decrease for $M293$. In $MM10$, it exhibits a moderate strength. (3) This abrupt feature becomes smooth and disappears when T is raised. (4) We identified a charge transfer from the top well to the bottom well at the transition in $M293$. These are very surprising results in that since the carrier density decreases continuously, no abrupt feature is expected.

A. Model based on single-particle picture

A theory based on the single-article Schrödinger equation is not likely to give any sudden feature when the sys-

tem changes from a double to a single layer. In order to confirm this, we performed a numerical analysis by solving the Schrödinger and Poisson equations self-consistently with changing the balance of the wells. We used a solver from Ref. 26. The results of the numerical analysis are shown in Figs. 4(a)–4(c) for the three samples as a function of ΔV_g (which is the difference in V_g from its value when densities are balanced). The result for

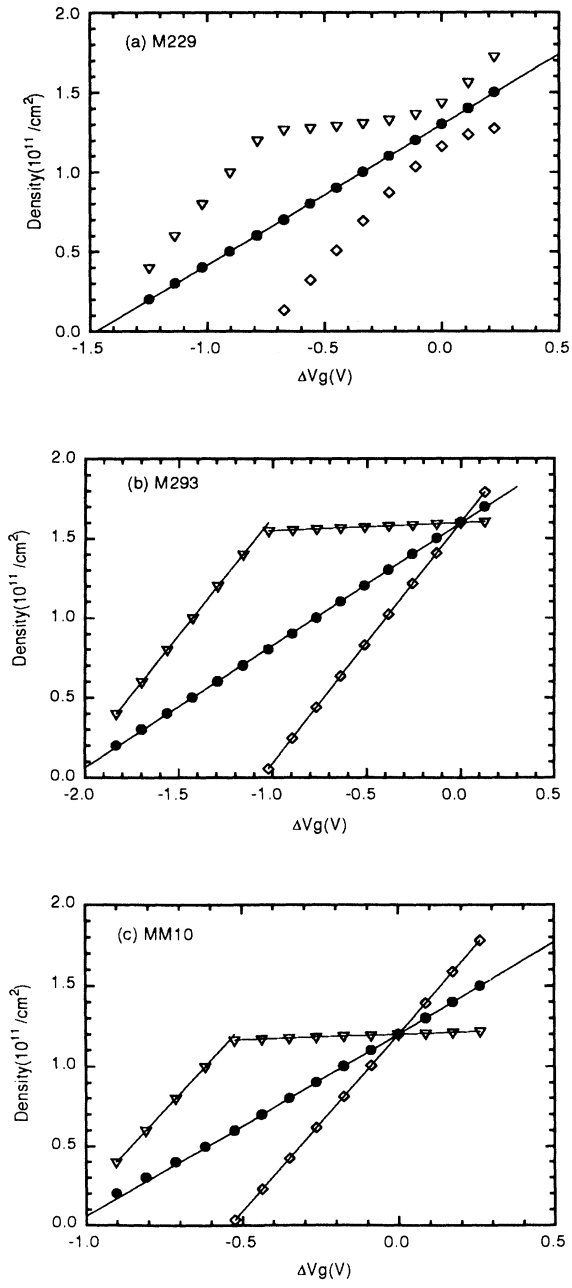

FIG. 4. Results of self-consistent calculation for three samples. Lines are linear fits: (a) $M229$; (b) $M293$; (c) $MM10$: ◇, n_1; ▽, n_2; ●, n_{av}.

$M229$ in Fig. 4(a) excellently reproduces the subband crossing in the experimental data in Fig. 3(a). The linear change in n_{av} also agrees with the experiment. The results for $M293$ in Fig. 4(b) do not show any sign of a sudden transition when the system is changed from a double-layer to a single-layer. The n's in the numerical analysis change linearly as a function of V_g and there is no sudden decrease in n_1, nor increase in n_2. The difference between the numerical analysis and the experimental data is apparent. The results for $MM10$ in Fig. 4(c) are similar to those for $M293$. There is no sign of charge transfer, even though the numerical analysis does not suffer from the low resolution problem due to the lower mobility of the sample in the experiment. Note that for $MM10$, the curvature change in n_{av} is noticeable after the top layer is depleted. The linearity observed in n_{av} for $M229$ and in all n's for $M293$ and $MM10$ shows that in this density range, the effect of Hartree potential is almost negligible. In other words, the circuit model,[25] which gives the linear dependence of n's, is as good an approximation as the self-consistent analysis. In conclusion, we cannot identify any signs of the sudden transition on the basis of the single-particle Schrödinger equation, even though the results of our analysis can well reproduce other features in the experimental data.

One might say that the abrupt feature in the experiment may be a result of a discontinuity in the density of state due to the upper subband depopulation.[27] However, in our case, this is not applicable. Since the energy difference between the quantum states in the individual wells is much larger than Δ_{SAS} for all three samples when the transition occurs, the upper and lower subbands are localized in the top and bottom wells. The spatial separation between the two subbands significantly reduces the electron scattering from one subband to the other. In addition, the resistance resonance in DQW's with large mobility imbalance when the wells are balanced[4,28] cannot be the cause of our resistance drop, since the wells in our DQW's are expected to have equal mobility and our resistance drop occurs far away from the balance condition.

B. Proposed model

We propose the following model based on the interlayer and intralayer correlations to explain the sudden transition. Since the purpose of the model is to provide a framework to explain qualitatively the strength of the transition for different samples, it is phenomenological in that we assume the matrix elements are given as a constant, and makes a simple estimation assuming weak coupling.

We start from the following model Hamiltonian:

$$\mathcal{H}=\sum_i \epsilon_0(a^\dagger_{1k_i}a_{1k_i}+a^\dagger_{2k_i}a_{2k_i})+\sum_i t(a^\dagger_{1k_i}a_{2k_i}+\text{H.c.}) + \sum_{i,j}\mathcal{U}(n_{1k_i}n_{ik_j}+n_{2k_i}n_{2k_j})+\sum_{i,j}\mathcal{V}n_{1k_i}n_{2k_j}\ , \quad (1)$$

where 1 and 2 are the layer index here and t, $\mathcal{U}$, and $\mathcal{V}$ are tunneling and the repulsive intralayer and interlayer Coulomb interactions, respectively; ϵ_0 is the kinetic ener-

gy, and H.c. stands for the Hermitian conjugate. We point out the similarity between our model and the multisubband Hubbard model which is extensively studied in the high-T_c superconductor literature.[13–17] In our case, the subbands are spatially separated and the in-plane wave function is not localized. In a simple approximation, the total energy of the system, E_{total}, which is the function to be minimized, may be written as

$$E_{\text{total}} \sim \epsilon_0(n_1+n_2)+t|n_1-n_2| + \mathcal{U}(n_1^2+n_2^2)+\mathcal{V}n_1n_2 , \quad (2)$$

where the second term on the right-hand side is the excess energy when the electrons are localized in one well compared to the case when electrons are in both wells. By substituting $n_1=n(\frac{1}{2}+\delta)$ and $n_2=n(\frac{1}{2}-\delta)$,

$$\frac{\delta E_{\text{total}}}{n^2}=(2\mathcal{U}-\mathcal{V})\delta^2+\frac{2t}{n}|\delta| . \quad (3)$$

Intuitively, the electron distribution is determined through the following competition: t and $\mathcal{U}$ try to distribute the electrons between the two wells while $\mathcal{V}$ tries to keep electrons in one well. Now there are three different cases: (*A*) $2\mathcal{U}-\mathcal{V}>0$, no instability; (*B*) $-4t/n<2\mathcal{U}-\mathcal{V}<0$, no instability; (*C*) $2\mathcal{U}-\mathcal{V}<-4t/n<0$, instability possible. Sample calculations of E_{total} for these cases are shown in Fig. 5. In both cases *A* and *B*, E_{total} is the smallest when $\delta=0$, since t and $\mathcal{U}$ win over $\mathcal{V}$. On the other hand, in case *C*, E_{total} at $\delta=\pm0.5$ is smaller than E_{total} at $\delta=0$, since $\mathcal{V}$ dominates.

The above model can give a qualitative explanation for the strength of the feature in the resistance and density data. First, considering the fact that the transition is the strongest for *M*293, the parameters for this sample have to satisfy case *C*. Second, since t changes exponentially as a function of the barrier width, while $\mathcal{V}$ changes algebraically,[5,29] t becomes much larger than $\mathcal{U}$ and $\mathcal{V}$ when the barrier becomes smaller. Therefore, the observed feature becomes weaker by approaching case *B*, consistent with our observation for sample *M*229. Third, if the barrier width is too large, t and $\mathcal{V}$ get reduced, so $\mathcal{U}$ becomes dominant. Again, the observed feature becomes weaker, on approaching case *A*, also consistent with our observing a weaker transition in *MM*10.

So far, the argument is qualitative. Let us study the case for *M*293 a little more quantitatively, following the calculation of the exchange-driven instability in DQW's by Ruden and Wu.[12] The effect of tunneling is ignored in the calculation. Even though the importance of tunneling should not be neglected in *M*229, ignoring tunneling is not a bad approximation for *M*293, which has a larger AlAs barrier. The reason $\mathcal{V}$ can be larger than $\mathcal{U}$ is that the latter can be greatly reduced due to the exchange effect, while the former can stay large since the wave functions overlap little in the z direction. In our case, when the wells are asymmetric, the total relevant energy of the system E_{total} can be written as

$$E_{\text{total}}=\tfrac{1}{2}\rho(E)^{-1}[(n_1-\Delta n)^2]-\rho(E)^{-1}(n_2-n_1)\Delta n + \frac{2\pi e^2}{\kappa_0}d\Delta n^2-\frac{4e^2}{3\kappa_0}\left[\frac{2}{\pi}\right]^{1/2} \times[(n_1-\Delta n)^{3/2}+(n_2+\Delta n)^{3/2}] , \quad (4)$$

where $\rho(E)$ is the two-dimensional density of states, κ_0 is the dielectric constant of the medium between the two 2DEG's, d is the distance between the 2DEG's, Δn is the density of the transferred electrons, and n_1, n_2 are the densities of the individual wells. Equation (4) has an additional term (the second term on the right-hand side) compared to the original formula in Ref. 12 due to the subband edge difference between the two wells. Figure 6 gives the calculated E_{total} normalized by $\rho(E)^{-1}n_2^2$ as a

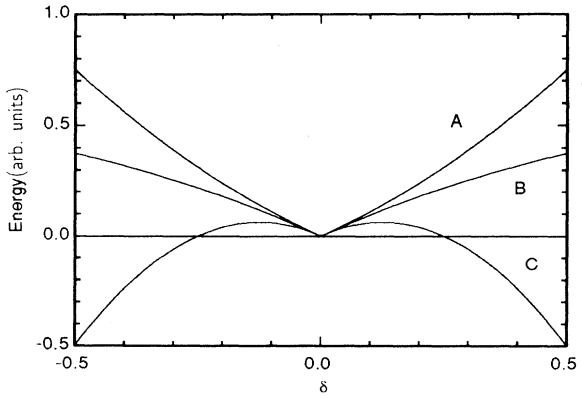

FIG. 5. Instability vs no instability; Case *A*, $2\mathcal{U}-\mathcal{V}=1$, $2t/n=1$; Case *B*, $2\mathcal{U}-\mathcal{V}=-0.5$, $2t/n=1$; Case *C*, $2\mathcal{U}-\mathcal{V}=04$, $2t/n=1$.

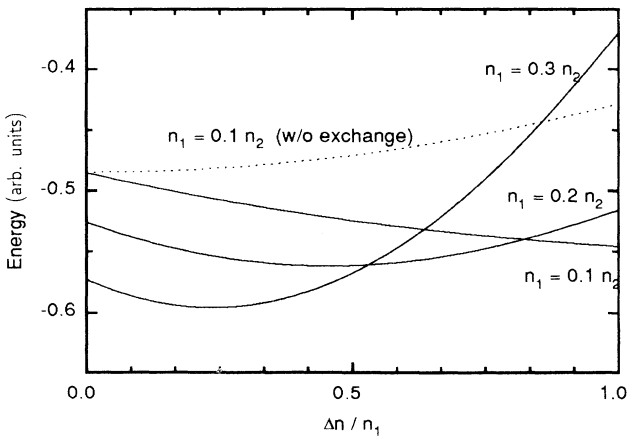

FIG. 6. The calculated total energy of the two 2DEG's as a function of the fractional density $\Delta n/n_1$ of electrons transferred from the top well to the bottom well for three different ratios of n_1 to n_2. We fix $n_2=1.4\times10^{11}/\text{cm}^2$. The dotted line is a calculation without the exchange term for $n_1=0.1n_2$ (y axis is shifted for comparison).

function of the transferred electron ratio $\Delta n/n_1$ for three different ratios of n_1 to n_2. We take $n_2=1.4\times10^{11}/\text{cm}^2$, $d=220$ Å, and $\kappa_0=12$. This calculation demonstrates that as n_1 decreases, more electrons in the top well are transferred to the bottom well due to the exchange interaction, consistent with our experimental findings.

C. Interlayer scattering

Now we study the interlayer scattering rate around the transition. The sudden resistance decrease is a result of the disappearance of the interlayer scattering due to the sudden top well depletion. A circuit model,[30] assuming the interlayer friction (which gives the interlayer resistance R_{12}) to be linear in the drift velocity difference between the wells, is used to estimate the interlayer scattering rate, τ_{12}, from the resistance data shown in Fig. 1(b). First, we fit the single-layer part ($V_g<-0.5$ V) of the data to a density-dependent layer resistance given by

$$R(n)=1/[8.1\times10^{-5}-0.0012(n/10^{11}) +0.009(n/10^{11})^2](\Omega)\ , \tag{5}$$

and approximate the resistances R_1 and R_2 of the top and bottom layers at a given V_g by the resistance $R(n_1)$ and $R(n_2)$ at the respective layer densities n_1 and n_2. Next, we extract R_{12} from the measured resistance

$$R^*_{\text{total}}=\frac{R^*_1R^*_2}{R^*_1+R^*_2}\ , \tag{6}$$

where

$$R^*_1=R_1+\frac{R_2[n_2/n_1]-R_1}{R_2[n_2/n_1]+2R_{12}[n_2/n_1]}R_{12}\left[\frac{n_2}{n_1}\right]\ , \tag{7}$$

and

$$R^*_2=R_2+\frac{R_1[n_1/n_2]-R_2}{R_1[n_1/n_2]+2R_{12}}R_{12}\ . \tag{8}$$

Finally, τ_{12} is calculated using $\tau_{12}=m^*/e^2n_2R_{12}$. The extracted R_{12}, which is the dashed curve in Fig. 7, increases as the system approaches the transition, and then shows a clear decrease and disappears at the transition. At $V_g=-0.44$ V, $R^*_{\text{total}}=100$ Ω, $n_1=0.2\times10^{11}/\text{cm}^2$, and $n_2=1.6\times10^{11}/\text{cm}^2$. We obtain $R_1=5000$ Ω and $R_2=48$ Ω. The estimated $R_{12}=60$ Ω, giving $\tau_{12}\sim2.5\times10^{-11}$ s at $T=0.3$ K. Note that since $R^*_{\text{total}}\to R_2+R_{12}$ when $R_1\to\infty$, a small uncertainty in R_1 around the peak of R_{12} will not affect the result much.

The interlayer scattering rate before the transition appears strongly enhanced when we compare our τ_{12} to the experimental[5] and theoretical[20] interlayer scattering rate known in the literature for higher densities far away from the transition. Gramila *et al.*[5] deduced an interlayer scattering time, $\tau_{12}\sim10^{-6}/T^2$ s, from a sample with an interlayer separation $d\sim200$ Å. Even if we scale this result according to

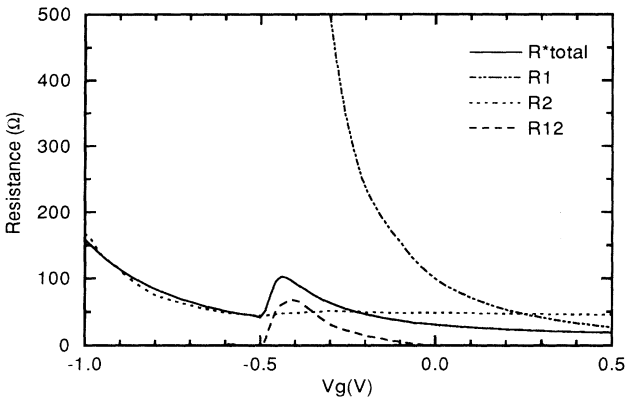

FIG. 7. R_{12} extracted from R^*_{total} taken at $T=0.3$ K on $M293$. R_1 and R_2 used in the calculation are also shown.

$$\tau_{12}\sim\frac{T^2}{E_F^2d^4}\ , \tag{9}$$

neglecting the finite width of the 2DEG's,[5,20] their $\tau_{12}\sim10^{-8}/T^2$ s, still more than three orders of magnitude larger than our value before the transition. The experiment on interlayer scattering between a 2DEG and a 3DEG by Solomon *et al.*[19] also gives a much smaller scattering rate. In other words, the interlayer scattering at the transition is significantly enhanced, when compared to that from the previous interlayer Coulomb scattering studies. In fact, its strength is comparable to that of the electron-hole system.[6]

Here we discuss some possibilities to explain this enhancement. The first and most likely possibility is weaker screening due to the low densities in the sample, in particular, when the top layer approaches depletion. We do a simple order of magnitude estimation of the interlayer Coulomb forces in the absence of the top-layer screening for $M293$, by comparing them to the Coulomb forces due to the remote donors. The electrons in the top well are an order of magnitude closer in distance to the bottom electron layer than to the remote donors (which is ~1000 Å away) and thus, the potential is an order of magnitude stronger,[31] but an order of magnitude less in density just before the transition (at $V_g=-0.44$ V, n_1 is estimated to be 13% of n_2). Therefore, the scattering rate of the bottom-layer electrons due to the electrons in the top layer is comparable to that due to the remote donors, if we assume a similar scattering mechanism. The amount of the resistance drop in our data is consistent with this estimation. Second, since the theory does not deal with the finite layer thickness of the real system, the extrapolation using Eq. (9) may not be accurate. The finite thickness cannot be neglected in our case, since the layer separation is much smaller than that used in the previous studies and is comparable to the thickness of the 2DEG's. The third possibility is the disorder enhancement of the interlayer scattering rate.[31] According to the theory, the interlayer Coulomb interaction is

appreciably enhanced by disorder at low T when the mean-free path within a layer is comparable to or shorter than the layer separation. However, this effect may not be large since at $V_g = -0.44$ V, the mean-free path in the top layer is ~ 1500 Å, which is still larger than the interlayer separation. Fourth, the interlayer scattering rate may be enhanced as a result of increasing fluctuations due to the instability. However, since the onset of the enhancement in R_{12} in our data occurs much earlier than the transition, such increasing fluctuations may not be the main reason for the enhancement.

V. CONCLUSION

In conclusion, we report detailed measurements of an abrupt transition from a double- to a single-layer system in the DQW's when the wells are biased. Of the three samples with different barrier widths (14, 70, and 100 Å) that we have studied, this transition is strongest for the 70-Å barrier width sample and disappears when temperature is raised. A phenomenological theory is developed within a framework of the charge transfer to explain the transition. We also find that the interlayer Coulomb scattering is significantly enhanced before the transition. Finally, we should mention that the layer degree of freedom in DQW's has also been identified with a pseudospin degree of freedom where the pure single-layer states are the eigenstates of the z component of the spin operator.[32] In this language, the transition that we have observed can be viewed as a field-induced paramagnetic to ferromagnetic transition.[33]

ACNOWLEDGMENTS

We acknowledge R. N. Bhatt for discussions. This work is supported in part by the MRG in Princeton University under NSF Grant No. DMR-9224077 and the ARO (Grant No. DAAH0493-G0071), and Y.K. acknowledges the financial support from the IBM Japan and H.C.M. from the Fannie and John Hertz Foundation.

*Present address: IBM Research, Tokyo Research Laboratory, 1623-14 Shimotsuruma, Yamato-shi, Kanagawa-ken 242, Japan.

[1]J. Smoliner, W. Demmerle, G. Berthold, E. Gornik, and G. Weimann, Phys. Rev. Lett. **63**, 2116 (1989).
[2]J. P. Eisenstein, L. N. Pfeiffer, and K. W. West, Appl. Phys. Lett. **58**, 1497 (1991).
[3]J. P. Eisenstein, L. N. Pfeiffer, and K. W. West, Phys. Rev. Lett. **28**, 3804 (1992).
[4]A. Palevski, F. Beltram, F. Capasso, L. Pfeiffer, and K. W. West, Phys. Rev. Lett. **65**, 1929 (1990).
[5]T. J. Gramila, J. P. Eisenstein, A. H. MacDonald, L. N. Pfeiffer, and K. W. West, Phys. Rev. Lett. **66**, 1216 (1991).
[6]U. Sivan, P. M. Solomon, and H. Shtrikman, Phys. Rev. Lett. **68**, 1196 (1992).
[7]G. S. Boebinger, H. W. Jiang, L. N. Pfeiffer, and K. W. West, Phys. Rev. Lett. **64**, 1793 (1990).
[8]S. Q. Murphy, J. P. Eisenstein, G. S. Boebinger, L. N. Pfeiffer, and K.W. West, Phys. Rev. Lett. **72**, 728 (1994).
[9]Y. W. Suen, L. W. Engel, M. Santos, M. Shayegan, and D. C. Tsui, Phys. Rev. Lett. **68**, 1379 (1992).
[10]J. P. Eisenstein, G. S. Boebinger, L. N. Pfeiffer, and S. He, Phys. Rev. Lett. **68**, 1383 (1992).
[11]A. H. MacDonald, Phys. Rev. B **37**, 4792 (1988).
[12]P. P. Ruden and Z. Wu, Appl. Phys. Lett. **59**, 2165 (1991).
[13]P. B. Littlewood, C. M. Varma, and E. Abrahams, Phys. Rev. Lett. **63**, 2602 (1989).
[14]P. B. Littlewood, Physica B **163**, 299 (1990).
[15]S. N. Coopersmith and P. B. Littlewood, Phys. Rev. B **41**, 2646 (1990).
[16]R. Putz, B. Ehlers, L. Lilly, A. Muramatsu, and W. Hanke, Phys. Rev. B **41**, 853 (1990).
[17]Y. Bang, G. Kotliar, C. Castellani, M. Grilli, and R. Raimondi, Phys. Rev. B **43**, 13724 (1991).
[18]The preliminary data can be found in Y. Katayama, D. C. Tsui, H. C. Manoharan, and M. Shayegan, Surf. Sci. **305**, 405 (1994).
[19]P. M. Solomon, P. J. Price, D. J. Frank, and D. C. L. Tulip, Phys. Rev. Lett. **63**, 2508 (1989).
[20]H. C. Tso and P. Vailopoulos, Phys. Rev. Lett. **68**, 2516 (1992).
[21]See, for example, C. Cohen-Tannoudji, B. Diu, and F. Laloë, *Quantum Mechanics* (Wiley-Interscience, New York, 1977).
[22]S. Luryi, Appl. Phys. Lett. **52**, 501 (1988).
[23]P. T. Coleridge, Semicond. Sci. Technol. **5**, 961 (1990).
[24]S. E. Schacham, E. J. Haugland, and S. A. A. Alterovitz, Phys. Rev. B **45**, 13 417 (1992).
[25]Y. Katayama and D. C. Tsui, Appl. Phys. Lett. **62**, 2563 (1993).
[26]S. Parihar, Ph.D. thesis, Princeton University, 1994.
[27]H. L. Stormer, A. C. Gossard, and W. Wiegmann, Solid State Commun. **41**, 707 (1982); Y. Ma, R. Fletcher, E. Zaremba, M. D'iorio, C. T. Foxon, and J. J. Harris, Surf. Sci. **229**, 80 (1990).
[28]Y. Ohno, M. Tsuchiya, T. Matsusue, T. Noda, and H. Sakaki, Surf. Sci. **305**, 322 (1994).
[29]L. Zheng and A. H. MacDonald, Phys. Rev. B **48**, 8203 (1993).
[30]Y. Katayama, Ph.D. thesis, Princeton University, 1994.
[31]A. L. Efros, Solid State Commun. **70**, 253 (1989).
[32]See, for example, A. H. MacDonald, P. M. Platzman, and G. S. Boebinger, Phys. Rev. Lett. **65**, 775 (1990).
[33]E. C. Stoner, Rep. Prog. Phys. **11**, 43 (1940); J. Phys. Radium **12**, 372 (1951).